

# Molecular Association in Binary Mixtures of *tert*-Butyl Alcohol–Water and Tetrahydrofuran–Heavy Water Studied by Mass Spectrometry of Clusters from Liquid Droplets

Toshiko Fukasawa,<sup>†</sup> Yasunori Tominaga,<sup>\*,†</sup> and Akihiro Wakisaka<sup>\*,‡</sup>

Department of Physics and Chemistry, Graduate School of Humanities and Sciences, Ochanomizu University, Otsuka, Bunkyo-ku, Tokyo 112-8610, Japan, and National Institute of Advanced Industrial Science and Technology, AIST, Tsukuba West, Onogawa 16-1, Tsukuba, Ibaraki 305-8569, Japan

Received: August 25, 2003

The cluster structures observed by means of mass spectrometry for binary mixtures—*tert*-butyl alcohol (TBA)—H<sub>2</sub>O and tetrahydrofuran (THF)—D<sub>2</sub>O—with varying mixing ratios exhibit striking contrast, even though both TBA and THF are miscible with water at any mixing ratio. In the TBA–H<sub>2</sub>O mixtures at TBA mole fractions of  $(X_{\text{TBA}}) \leq 0.01$ – $0.025$ , some of the H<sub>2</sub>O molecules in the H<sub>2</sub>O clusters are replaced by TBA molecules. For  $0.01$ – $0.025 \leq X_{\text{TBA}} \leq 0.2$ – $0.3$ , the self-aggregation of TBA forms dominant cluster structures, and the hydrogen-bonded water clusters are disintegrated with increasing  $X_{\text{TBA}}$ . This TBA self-aggregation is reduced with further increasing TBA at  $X_{\text{TBA}} \geq 0.3$ . However, in the THF–D<sub>2</sub>O mixtures, THF molecules have a weak additional interaction with D<sub>2</sub>O clusters, and the self-aggregation of THF is not promoted in the THF–D<sub>2</sub>O mixtures. The D<sub>2</sub>O clusters still exist, even at a THF mole fraction of  $X_{\text{THF}} = 0.3$ . On the basis of the observed cluster structure, the mechanism for the mixing between water and the organic solvent and the controlling factors in the self-aggregation are proposed.

## Introduction

Even though an organic solvent is miscible with water, the intermolecular interactions of water–water, water–organic molecule, and organic molecule–organic molecule are not the same. The interaction between water and the hydrophobic group of the organic solvent molecule should be especially weak in the mixtures. As a result of the balance of these intermolecular interactions in the water–organic solvent mixture, clusters will be formed easily in the mixture.

Because organic molecules have different kinds of intermolecular interactions in their aqueous solutions, we confine our focus to *tert*-butyl alcohol (TBA) and tetrahydrofuran (THF) because TBA has an OH group but THF does not. Although both of them are miscible with water at any mixing ratio, the balance of intermolecular interactions in a TBA–water mixture should be quite different from that in a THF–water mixture. This will lead to the difference in the cluster structure.

Many investigations have been performed on physical and chemical properties of the TBA–water<sup>1–4,7,8</sup> and THF–water mixtures<sup>5–8</sup> through various experimental and theoretical approaches. It has been concluded that the characteristic microscopic structure in these mixtures in a water-rich region is a cage structure of water molecules around TBA and THF molecules. However, the difference in the intermolecular interactions between TBA–water and THF–water was not exactly reflected in the reported results. Here we report how the difference in the intermolecular interactions is reflected in the cluster structure observed through the mass spectrometric

analysis of clusters isolated from liquid droplets. The resulting information on the cluster structures in these binary mixtures also shows the difference in the way of mixing at the molecular level.

## Experimental Section

The mass spectra of clusters generated from liquid droplets were measured by a specially designed mass spectrometer. This original design was proposed by Nishi.<sup>9,10</sup> The details have been provided elsewhere.<sup>9–12</sup> The spectrometer consists of a heated nozzle, a quadrupole mass filter (Extrel C50-4000), and a four-stage differentially pumped vacuum system divided by the skimmers. A sample solution was injected into the first chamber ( $10^{-1}$  Torr) through the heated nozzle (160–155 °C) with a flow rate of 0.12 mL/min by using a liquid chromatograph pump (Shimadzu, LC-10AD). The nozzle was heated electrically to form a flow of liquid droplets against the decrease in temperature due to the vaporization, and its temperature was monitored and controlled by two sets of thermocouples on the nozzle. When a part of the solution is vaporized in the nozzle, the resulting gas–liquid mixtures form a flow of liquid droplets. The temperature of the liquid droplets should be much lower than the nozzle temperature. This temperature difference was estimated to be 70–90 °C.<sup>9,10</sup> Owing to the pressure gradient, the resulting liquid droplets are led to the second ( $10^{-3}$  Torr) and the third ( $10^{-5}$  Torr) chamber, which leads to the fragmentation of the liquid droplets into clusters via adiabatic expansion. The mass spectra of the clusters were measured by the quadrupole mass filter after an electron-impact ionization with 30.1 eV.

The pure water was prepared by Milli-Q SP. TOC (Millipore). The TBA (99.0%, Wako), THF (99.5%, no stabilizer, Wako), and D<sub>2</sub>O (99.9%, Aldrich) were used without further purification. The concentrations of the sample solutions were expressed

\* To whom correspondence should be sent. A.W. E-mail: akihiro-wakisaka@aist.go.jp. Y.T. E-mail: tominaga@phys.ocha.ac.jp.

<sup>†</sup> Ochanomizu University.

<sup>‡</sup> National Institute of Advanced Industrial Science and Technology.

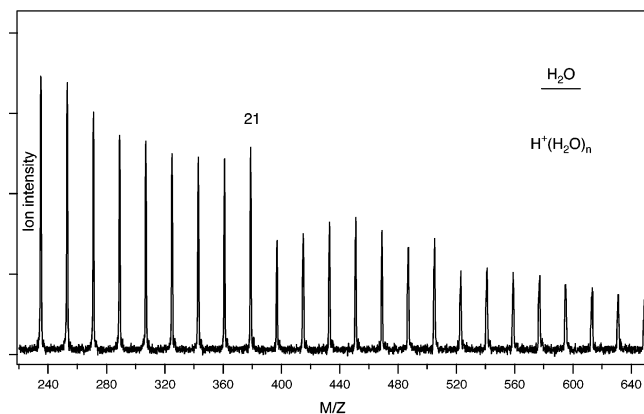


**Figure 1.** Mass spectrum for clusters generated from pure water ( $\text{H}_2\text{O}$ ). The numbers written on the peaks represent  $n$  for  $\text{H}^+(\text{H}_2\text{O})_n$ .

by TBA mole fractions ( $X_{\text{TBA}}$ ) and THF mole fractions ( $X_{\text{THF}}$ ):  $X_{\text{TBA}} = 0.0, 0.0024, 0.005, 0.0075, 0.01, 0.025, 0.05, 0.1, 0.2, 0.3, 0.4$ ;  $X_{\text{THF}} = 0.0, 0.01, 0.05, 0.1, 0.2, 0.3, 0.6, 0.8$ .

## Results

**1. TBA–Water Binary Mixtures.** It was observed through mass spectrometry that the cluster structures in TBA–water mixtures varied remarkably depending on the TBA mole fraction ( $X_{\text{TBA}}$ ). We could classify the TBA–water mixtures into three regions according to the observed cluster structures as follows: region A ( $0 \leq X_{\text{TBA}} \leq 0.01$ – $0.025$ ), region B ( $0.01$ – $0.025 \leq X_{\text{TBA}} \leq 0.2$ – $0.3$ ), and region C ( $0.3 \leq X_{\text{TBA}}$ ). The representative mass spectrum of each region is shown below.

*Region A* ( $0 \leq X_{\text{TBA}} \leq 0.01$ – $0.025$ ). The mass spectrum of clusters for pure water ( $X_{\text{TBA}} = 0$ ) is shown in Figure 1. The hydrogen-bonded water clusters,  $\text{H}^+(\text{H}_2\text{O})_n$ , are observed as a series of clusters. This mass distribution is very reproducible and in good agreement with the reported results.<sup>11,12</sup> Although  $\text{H}^+(\text{H}_2\text{O})_n$  clusters from  $n = 1$ – $50$  were observed, the sensitivity and the resolution get worse in lower- and higher-mass regions, respectively. Furthermore, in lower-mass regions, fragmented clusters from larger clusters might be included. To avoid these influences, the region shown in each Figure was focused here. Some peaks are observed as the prominent peaks compared with their neighboring ones. The most representative one is the peak of  $\text{H}^+(\text{H}_2\text{O})_{21}$ , which is called “magic number species.” The magic number property indicates that more stable structure is included as one of the isomers. It should be noted here that the formation of magic number species reflects the stability after fragmentation of clusters via electron impact ionization. Therefore, the magic number anomaly does not reflect the mass distribution in the solution. However, when a sample solution such as a TBA–water mixture has the same hydrogen bonding network of water as that in the pure water, the mass distribution including the magic number species will be always observed. Here we use the magic number property as an index which reflects the clustering structure of the pure water.

At  $0 \leq X_{\text{TBA}} \leq 0.01 \sim 0.025$ , the hydrogen-bonded water clusters,  $\text{H}^+(\text{H}_2\text{O})_n$ , as observed in pure water (Figure 1), compose a main structure in the molecular clustering. Figure 2a shows a mass spectrum of clusters generated from a solution at  $X_{\text{TBA}} = 0.0024$ . In addition to the series of water clusters, TBA hydrate clusters,  $\text{H}^+(\text{TBA})_m(\text{H}_2\text{O})_n$ :  $m = 1 \sim 5$ , are observed as a series of clusters in this region A. The blue, red, yellow, and green lines in Figure 2a correspond to the cluster series of  $\text{H}^+(\text{H}_2\text{O})_n$ ,  $\text{H}^+(\text{TBA})_1(\text{H}_2\text{O})_n$ ,  $\text{H}^+(\text{TBA})_2(\text{H}_2\text{O})_n$ , and  $\text{H}^+(\text{TBA})_3(\text{H}_2\text{O})_n$ , respectively. When we focus on the series

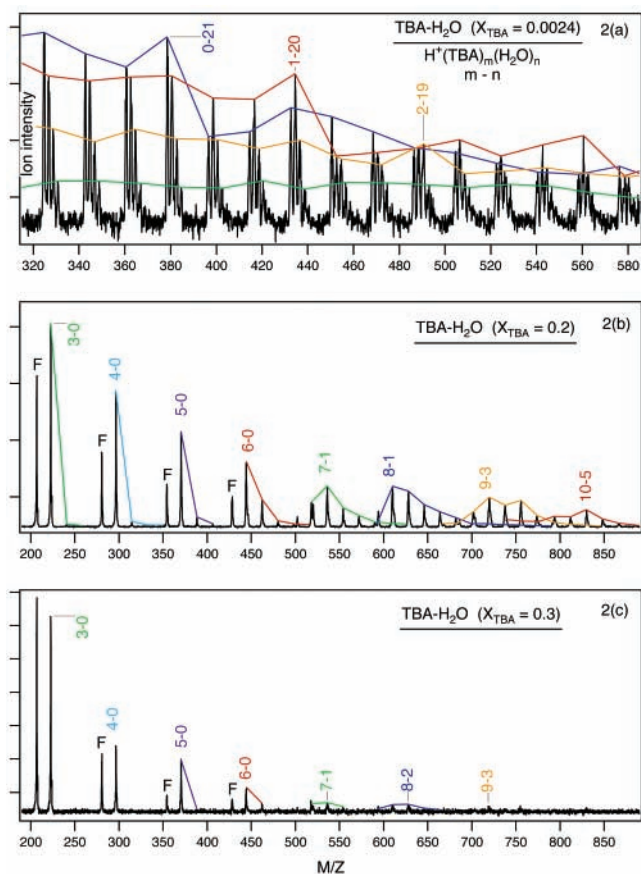


**Figure 2.** Mass spectra for clusters generated from *tert*-butyl alcohol (TBA)– $\text{H}_2\text{O}$  mixtures. The paired numbers represent  $m$ – $n$  for  $\text{H}^+(\text{TBA})_m(\text{H}_2\text{O})_n$ . The peaks with the same number of TBA ( $m$ ) are connected by the colored lines. The blue, red, yellow, and green lines correspond to the cluster series of  $\text{H}^+(\text{H}_2\text{O})_n$ ,  $\text{H}^+(\text{TBA})_1(\text{H}_2\text{O})_n$ ,  $\text{H}^+(\text{TBA})_2(\text{H}_2\text{O})_n$ ,  $\text{H}^+(\text{TBA})_3(\text{H}_2\text{O})_n$ , respectively. The peaks labeled with F represent the clusters including a fragmented TBA molecule. (a)  $X_{\text{TBA}} = 0.0024$ , (b)  $X_{\text{TBA}} = 0.2$ , (c)  $X_{\text{TBA}} = 0.3$ .

of clusters composed of the same number of TBA molecules ( $m$ ) and the varying number of water molecules ( $n$ ), as shown by the connected lines in Figure 2a, each series of clusters is found to show mass distribution similar to that for the pure water. This indicates that the hydrogen-bonding network of water is not influenced by the mixing with TBA in this region A. Accordingly, the magic number species are also observed in each series of TBA hydrate clusters, but the number of water molecules varies to satisfy  $m + n = 21$  for  $\text{H}^+(\text{TBA})_m(\text{H}_2\text{O})_n$  clusters. In Figure 2a, the TBA hydrate clusters,  $\text{H}^+(\text{TBA})_m(\text{H}_2\text{O})_n$  represented by  $m$ – $n$ , show magic number property at 1–20 and 2–19. In addition to the magic number property, the mass distribution of each series of cluster is similar to that of the pure water. Therefore, the TBA molecule can have substitutional interaction with not only the magic number cluster but also with all the water clusters in the region A.

*Region B* ( $0.01 \sim 0.025 \leq X_{\text{TBA}} \leq 0.2 \sim 0.3$ ). In region B, the TBA self-aggregation clusters form prominently instead of the water clusters. Figure 2b shows a mass spectrum of the solution of  $X_{\text{TBA}} = 0.2$ , as a typical one in the region B. In the clusters  $\text{H}^+(\text{TBA})_m(\text{H}_2\text{O})_n$  represented by  $m$ – $n$ , 3–0, 4–0, 5–0, and 6–0 are prominent in the relatively small clusters, while 7–1, 8–1, 9–3, and 10–5 are prominent in the relatively large clusters. The TBA self-aggregation clusters,  $\text{H}^+(\text{TBA})_m$ :  $m \leq 6$ , are stable, but those with  $m \geq 7$  are stabilized by including water molecules. As for the large clusters  $\text{H}^+(\text{TBA})_m(\text{H}_2\text{O})_n$ :

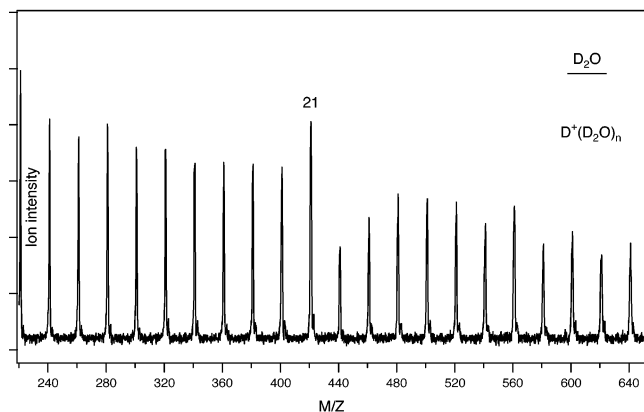


**Figure 3.** Mass spectrum for clusters generated from pure heavy water ( $D_2O$ ). The numbers written on the peaks represent  $n$  for  $D^+(D_2O)_n$ .

$m = \sim 10$ , we insist that the water molecules are incorporated into the hydrogen-bonding network of TBA. The TBA large clusters can exist stably only with existing water molecules, because water molecules adhere TBA molecules by hydrogen bonding.

**Region C** ( $0.3 \leq X_{TBA}$ ). In region C, the self-aggregation of TBA promoted by the presence of water, as observed in region B, was obviously reduced with an increase of  $X_{TBA}$ . A typical mass spectrum, observed for  $X_{TBA} = 0.3$ , is shown in Figure 2c. The self-aggregation clusters  $H^+(TBA)_m$  with  $m \geq 4$  are difficult to form. The  $H^+(TBA)_m(H_2O)_n$  clusters with  $m \geq 7$  are also decreased markedly. At  $X_{TBA} = 0.4$ , the clusters larger than  $H^+(TBA)_3$  were hardly formed. It is interesting that the large clusters,  $H^+(TBA)_m$  with  $m \geq 4$ , are observed in the system with higher water contents.

**2. THF–Heavy Water Binary Mixtures.** In THF–heavy water mixtures, the observed cluster structures are in good contrast to those in the TBA–water mixtures. We used heavy water instead of normal water for the measurement of the THF–water binary mixtures, because the mass number of a THF molecule equals that of  $H_2O$  tetramer. We were able to distinguish hydrated THF from heavy water clusters clearly.

The mass spectrum of clusters generated from heavy water ( $X_{THF} = 0$ ) is shown in Figure 3, and it is quite similar to that for normal water (Figure 1), except the difference in mass number between  $H_2O$  and  $D_2O$ .

When THF is added to heavy water up to the THF mole fraction,  $X_{THF} = 0.3$ , the water cluster structure is maintained with almost the same mass distribution as observed in pure heavy water. It is claimed that this may be related to the hydrogen bonding interaction among  $D_2O$  molecules being stronger than that among  $H_2O$  molecules. We have also confirmed that the water cluster structure is maintained in THF– $H_2O$  ( $X_{THF} = 0.3$ ), as observed in the pure water, even though the several peaks are overlapped. This indicates that the difference between  $D_2O$  and  $H_2O$  does not influence the observed cluster structures. The mass spectra representative of the THF– $D_2O$  mixtures are shown in Figure 4. The blue, red, and yellow lines in Figure 4 correspond to the cluster series of  $D^+(D_2O)_n$ ,  $D^+(THF)_1(D_2O)_n$ , and  $D^+(THF)_2(D_2O)_n$ , respectively. At  $X_{THF} = 0.05$  (Figure 4a), water clusters,  $D^+(D_2O)_n$ , are observed dominantly, and THF monomer and its hydrate clusters,  $D^+(THF)_1(D_2O)_n$ , are also observed. The peak intensities of  $D^+(THF)_1(D_2O)_n$  are quite weak compared with those of the water clusters and the THF monomer. With an increase of the THF concentration to  $X_{THF} = 0.2$  and  $0.3$ , the intensity of  $D^+(THF)_1(D_2O)_n$  increases gradually, as observed in Figure

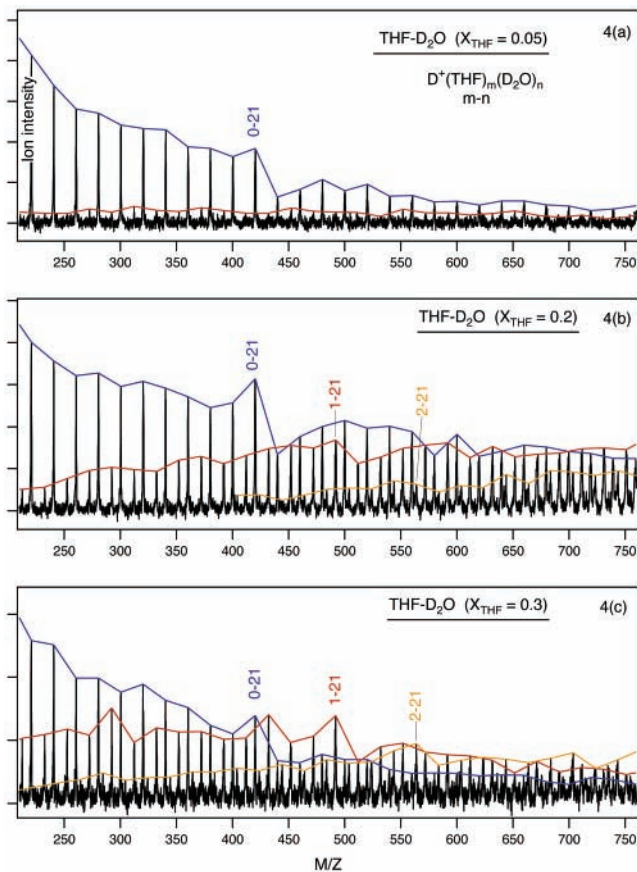


**Figure 4.** Mass spectra for clusters generated from tetrahydrofuran (THF)– $D_2O$  mixtures. The paired numbers represent  $m-n$  for  $D^+(THF)_m(D_2O)_n$ . The peaks with the same number of THF ( $m$ ) are connected by the colored lines. The blue, red, and yellow lines correspond to the cluster series of  $D^+(D_2O)_n$ ,  $D^+(THF)_1(D_2O)_n$ , and  $D^+(THF)_2(D_2O)_n$ , respectively. (a)  $X_{THF} = 0.05$ , (b)  $X_{THF} = 0.2$ , (c)  $X_{THF} = 0.3$ .

4b and c, respectively. The  $D^+(THF)_2(D_2O)_n$  are also observed in Figure 4b and c. THF dimer without  $D_2O$  molecules cannot be observed, and the peak intensity of THF dimer hydrate clusters with a few water molecules are extremely weak. For the THF hydrate cluster series,  $D^+(THF)_m(D_2O)_n$ ,  $m = 1$  and  $2$ , especially for  $m = 2$ , the intensities of relatively large clusters increase with increasing THF concentration. This suggests that THF molecules might exist in the space among the water clusters.

Furthermore, we have confirmed that the clusters,  $D^+(THF)_m(D_2O)_n$ ;  $m-n = 1-21$  and  $2-21$ , are observed as magic-number species in Figure 4b and c. The  $D^+(THF)_m(D_2O)_n$  clusters with  $n = 21$  show the magic number property, irrespective of the number of THF molecules in the cluster. This indicates that THF molecules have additional interaction with  $D_2O$  clusters. This is obviously different from the TBA–water substitutional interaction. Such an additional interaction between THF and water clusters will make the hydrogen-bonded  $D_2O$  clusters maintained even at  $X_{THF} = 0.3$ , as shown in Figure 4c. The self-aggregation of THF, as observed in the TBA– $H_2O$  mixtures, is hardly promoted in the THF– $D_2O$  binary mixtures.

At  $X_{THF} \geq 0.6$ , the peak intensities of  $D_2O$  clusters decreased and the size of  $D_2O$  clusters became small. Their mass distributions are different from that in pure  $D_2O$ . The hydrogen-bonding network of  $D_2O$  is disintegrated in this higher  $X_{THF}$ . The  $D^+(THF)_m(D_2O)_n$  also decreases with increasing  $X_{THF}$  and was hardly observed at  $X_{THF} = 0.8$ .



## Discussion

**1. Difference in the Molecular Association.** Both TBA and THF are miscible with water at any mixing ratio. However, the mass spectrometric analysis of clusters in these mixtures demonstrated that the molecular association found in the THF–D<sub>2</sub>O system is very much different from the case in the TBA–H<sub>2</sub>O system.

In TBA–H<sub>2</sub>O mixtures (Figure 2), the water cluster structures are easily disintegrated by the addition of TBA, and the TBA self-aggregation clusters are formed instead of the water clusters. Such kind of microscopic change takes place even at the low TBA mole fraction ( $X_{\text{TBA}} = 0.01 \sim 0.025$ ). On the other hand, in THF–D<sub>2</sub>O mixtures (Figure 4), the water cluster structures are maintained even at  $X_{\text{THF}} = 0.3$ , as observed for  $\text{D}^+(\text{D}_2\text{O})_n$  and  $\text{D}^+(\text{THF})_{1,2}(\text{D}_2\text{O})_n$ , and the THF self-aggregation is not promoted by the addition of D<sub>2</sub>O. In both mixtures, when one component forms self-aggregation clusters, the other component is broken up to the monomeric molecules to maintain single phase as stably as possible. The same kind of difference in the cluster structure has been also observed between methanol–water and acetonitrile–water binary mixtures.<sup>11</sup> Accordingly, it should be noted that the cluster structures observed herein TBA–water and THF–water show representative two types of mixing mechanism between water and organic solvents.

**2. Controlling Factors in Cluster Formation.** In TBA–H<sub>2</sub>O mixtures, the stabilization for the hydrogen-bonding interactions H<sub>2</sub>O–H<sub>2</sub>O, H<sub>2</sub>O–TBA, and TBA–TBA will be comparable, but the interaction of the large alkyl group of TBA with H<sub>2</sub>O cannot provide stabilization. Therefore, the TBA self-aggregation is promoted by the increase of  $X_{\text{TBA}}$ , to complement the loss of stabilization caused by the contact of TBA with H<sub>2</sub>O. In region B ( $0.01 \sim 0.025 \leq X_{\text{TBA}} \leq 0.2 \sim 0.3$ ), each TBA molecule will have contact with the water molecules; therefore, the TBA–TBA interaction becomes relatively more stable than the TBA–H<sub>2</sub>O interaction working at the same time. This will induce the TBA self-aggregation. However, in region C, since the TBA molecules that do not contact water molecules increase with increasing  $X_{\text{TBA}}$ , the relative stability for the TBA–TBA interaction against the TBA–H<sub>2</sub>O interaction disappears with increasing  $X_{\text{TBA}}$ . It should be noted that the clustering of TBA is promoted in the presence of water, because it is controlled by the relative stability in the solution. In pure TBA, all TBA–TBA interaction is comparable, which cannot promote self-aggregation.

On the other hand, in THF–D<sub>2</sub>O mixtures, the D<sub>2</sub>O–D<sub>2</sub>O interaction energy is much larger than the THF–THF interaction energy. Accordingly, D<sub>2</sub>O clusters are maintained, and THF molecules should be surrounding the D<sub>2</sub>O clusters.

Since there are several intermolecular interactions working at the same time in the binary mixtures, the difference in the clustering between TBA–water and THF–water mixture will be explained by the balance of interactions rather than the absolute interaction energy.

**3. Correlation with Other Experimental and Theoretical Approaches.** The resulting concentration effect on the TBA self-aggregation is in good correlation with the reported IR, X-ray scattering, computer simulation, and thermodynamic studies.

(i) *IR.* Infrared studies for TBA–water mixtures revealed the changes of the TBA C–H stretching band in the 3200–2800 cm<sup>-1</sup> frequency region as depending on the mixing ratio.<sup>13</sup> It was observed that when the TBA concentration exceeds a critical concentration around  $X_{\text{TBA}} \sim 0.025$ , the C–H stretching band shifts to lower frequency with increase of  $X_{\text{TBA}}$ , while the C–H

stretching band keeps constant in  $X_{\text{TBA}} \leq 0.025$ . From this it was concluded that the shift of the C–H stretching band to the lower frequency region was due to the depletion of the aqueous environment around the TBA methyl group. This IR result can be connected to self-aggregation of TBA molecules observed through the mass spectrometry here. The mass spectra for the mixtures in the present study vary with increasing TBA concentration, but the changes are not linearly dependent on the TBA concentration. At  $X_{\text{TBA}} = 0.01$ , the peaks of the TBA self-aggregation clusters become obvious, but the TBA hydrated clusters and water clusters coexist. At  $X_{\text{TBA}} = 0.025$ , however, TBA self-aggregation clusters form prominently instead of the water clusters. The critical concentration between the region A and B, at  $X_{\text{TBA}} = 0.01 \sim 0.025$ , obtained through present mass spectrometric analysis for the cluster structures, is in good correlation with the critical concentration suggested by the IR studies.

(ii) *X-ray Scattering.* Small-angle X-ray scattering study showed that a large concentration fluctuation for TBA–water mixtures is enhanced strongly at  $X_{\text{TBA}} = 0.14 \sim 0.17$ .<sup>2</sup> It is suggested that heterogeneous mixing is most enhanced at this mixing ratio. This  $X_{\text{TBA}}$  value is in region B, proposed here by mass spectrometry. We have also observed that the self-aggregation of TBA is enhanced most markedly at  $X_{\text{TBA}}$  from 0.1 to 0.2. From this correlation, the concentration fluctuation is attributed to the self-aggregation of TBA molecules in the mixtures.

(iii) *Computer Simulation.* Computer simulation for TBA–water mixtures has been carried out on the site–site radial distribution function over the whole concentration range of TBA mole fraction.<sup>3</sup> It was concluded that, in concentrated TBA, TBA molecules were associated into the zigzag-like hydrogen-bonding chains of TBA and that the hydrophobic attraction of the bulky *tert*-butyl groups in aqueous solutions was performed for approximately 3 to 6 TBA molecules. These findings agree well with the present result shown in Figure 2b, where the TBA self-aggregation clusters larger than  $\text{H}^+(\text{TBA})_7$  incorporated with H<sub>2</sub>O. Also, self-aggregation clusters of TBA can be formed up to  $\text{H}^+(\text{TBA})_6$  without water molecules.

(iv) *Thermodynamic Properties.* Although the thermodynamic properties for TBA–H<sub>2</sub>O and THF–H<sub>2</sub>O binary mixtures look similar, the microscopic structures of TBA–H<sub>2</sub>O mixtures are in good contrast with those of THF–D<sub>2</sub>O mixtures. The excess molar enthalpies ( $H^E$ ) of TBA–H<sub>2</sub>O and THF–H<sub>2</sub>O solutions are both negative in  $X_{\text{TBA}} \leq 0.5$  and  $X_{\text{THF}} \leq 0.6$ , and they are both positive in  $X_{\text{TBA}} \geq 0.5$  and  $X_{\text{THF}} \geq 0.6$ .<sup>4,6</sup> In the region of negative  $H^E$ , the self-aggregation of one component molecules is promoted. TBA and D<sub>2</sub>O formed self-aggregation clusters in TBA–H<sub>2</sub>O and THF–D<sub>2</sub>O mixtures, respectively. This was controlled by the relatively large interaction energy. On the other hand, in the regions of positive  $H^E$ , the self-aggregation clusters disintegrated to afford more random mixing with the other component.

**Acknowledgment.** This work is partly supported by a Grant-in-Aid for Scientific Research from the Japanese Ministry of Education, Science, Culture, and Sport.

## References and Notes

- (1) Iwasaki, K.; Fujiyama, T. *J. Phys. Chem.* **1977**, *81*, 1908–1912.
- (2) Nishikawa, K.; Hayashi, H.; Iijima, T. *J. Phys. Chem.* **1989**, *93*, 6559–6565.
- (3) Yoshida, K.; Yamaguchi, T.; Kovalenko, A.; Hirata, F. *J. Phys. Chem. B* **2002**, *106*, 5042–5049.

- (4) Koga, Y. *Can. J. Chem.* **1988**, *66*, 3171–3175.
- (5) Takamuku, T.; Nakamizo, A.; Tabata, M.; Yoshida, K.; Yamaguchi, T.; Otomo, T. *J. Mol. Liq.* **2002**, *103–104*, 143–159.
- (6) Atkinson, G.; Rajagopalan, S.; Atkinson, B. L. *J. Phys. Chem.* **1981**, *85*, 733–739.
- (7) Matteoli, E.; Lepori, L. *J. Phys. Chem.* **1984**, *80*, 2856–2863.
- (8) Baumgartner, E. K.; Atkinson, G. *J. Phys. Chem.* **1971**, *75*, 2336–2341.
- (9) Nishi, N.; Yamamoto, K. *J. Am. Chem. Soc.* **1987**, *109*, 7353–7361.
- (10) Yamamoto, K.; Nishi, N. *J. Am. Chem. Soc.* **1990**, *112*, 549–558.
- (11) Wakisaka, A.; Abdoul-Carime, H.; Yamamoto, Y.; Kiyozumi, Y. *J. Chem. Soc., Faraday Trans.* **1998**, *94*, 369–374.
- (12) Wakisaka, A.; Komatsu, S.; Usui, Y. *J. Mol. Liq.* **2001**, *90*, 175–184.
- (13) Freda, M.; Onori, G.; Santucci, A. *J. Phys. Chem. B* **2001**, *105*, 12714–12718.